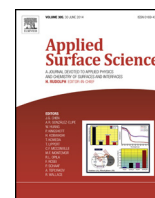




Contents lists available at ScienceDirect

Applied Surface Science

journal homepage: www.elsevier.com/locate/apsusc



The effect of post-annealing on Indium Tin Oxide thin films by magnetron sputtering method

J.H. Park^{a,*}, C. Buurma^a, S. Sivananthan^a, R. Kodama^b, W. Gao^b, T.A. Gessert^c

^a Department of Physics, University of Illinois at Chicago, 845 West Taylor Street, Chicago, IL 60607-7059, USA

^b EPIR Technologies, Inc., 590 Territorial Drive, Unit B, Bolingbrook, IL 60440, USA

^c National Renewable Energy Laboratory, Golden, CO 80401, USA

ARTICLE INFO

Article history:

Received 6 September 2013

Received in revised form 28 February 2014

Accepted 6 April 2014

Available online xxx

PACS:

61.72.Cc

71.20.Nr

78.20.Ci

81.15.Cd

82.80.Pv

Keywords:

ITO

Post-annealing

Bandgap

XPS

ABSTRACT

We report effects of post-annealing on Indium Tin Oxide (ITO) thin films by their physical, electrical, optical, and electronic properties. Carrier concentrations increase up to annealing temperatures of 400 °C, and then decrease at higher annealing temperatures. Burstein–Moss effect occurs as a function of annealing temperature with the highest optical bandgap of 4.17 eV achieved at 400 °C. X-ray photoelectron spectroscopy revealed a ~0.3 eV shift in the Fermi level of the annealed ITO films at 400 °C, and the shift was reduced for temperatures higher than 400 °C. In addition, the results of curve-fitting for the core levels showed a change of ratios of SnO₂ and oxygen in the oxygen deficient regions after annealing. This is correlated to the change of carrier concentration and optical bandgap in the ultraviolet and near-infrared regions at different annealing temperatures.

© 2014 Elsevier B.V. All rights reserved.

1. Introduction

For most optoelectronic devices such as flat panel-displays, light-emitting diodes and photovoltaic solar cells, transparent conducting oxide (TCO) thin films play an important role as a transparent electrode [1–3]. Although there are a large number of different TCOs including some multi-components oxides and ternary compounds, impurity-doped In₂O₃, ZnO, and SnO₂ are the most common in practical use [4]. Especially, Sn-doped In₂O₃ (ITO) has been widely studied for over 40 years and is often preferred due to its high electrical and optical qualities [5]. Despite an extensive research effort into ITO with the other TCOs, significant questions remain regarding the effects that defects, growth conditions, and post treatment have on film properties [6–8]. Furthermore, the carrier concentration dependence of the bandgap shift (by Burstein–Moss effect and bandgap renormalization) is still not well understood for ITO films as well as for other TCOs due to a mismatch between theoretical models and experimental data

[9,10]. Because the properties of conductivity and transmittance for most TCOs can be affected by this carrier concentration, it is very important to understand the nature of dopants and defects, especially for high-performance optoelectronic devices. In this letter, we explore changes to the electrical and optical properties of ITO thin films deposited by magnetron sputtering due to post-deposition annealing.

2. Experimental procedure

ITO films were prepared on quartz substrates by radio-frequency (r.f.) magnetron sputtering using 2-inch-diameter ITO target (10 wt.% SnO₂). The ITO target was produced by Nikko Metals USA, Inc. (Chandler, AZ) and was 99.99% pure. All 16 substrates (12.7 mm × 12.7 mm each) were loaded on a single holder after a standard solvent clean, and the system was pumped to 1.1×10^{-7} Torr with a turbo pump. Sputtering was performed in a custom designed unit hitherto referred to as (MPL-S) at room temperature in pure Ar, at a throttled pressure of 4 mTorr and at 120 Watts (10 sccm Ar flow, pressure measured with a capacitance manometer). Substrate rotation provided to enhance deposit uniformity. The ITO films were ex situ annealed under nitrogen gas

* Corresponding author. Tel.: +1 3126623878; fax: +1 3129969016.
E-mail addresses: jpark217@uic.edu, fishperson99@gmail.com (J.H. Park).

Table 1
Surface roughness for the as-grown and post-annealed ITO films.

	As-grown	250 °C	300 °C	350 °C	400 °C	450 °C	500 °C	550 °C
Surface roughness	1.64 nm	1.93 nm	2.01 nm	2.35 nm	2.57 nm	2.28 nm	2.20 nm	2.18 nm

flow (~420 sccm) in a tube furnace at various temperatures from 250 °C to 550 °C for 30 min (two samples at each temperature).

The thickness of the ~150 nm films was obtained using stylus profilometer (Ambios Technology XP-1). The variation of thickness for the annealed films was less than ~7 nm (maximum 4 nm and minimum -7 nm) with respect to the thickness for the as-grown films. The crystallographic structure of the as-grown and post-annealed ITO films was analyzed by X-ray diffraction (XRD) using a Bede D1 system (Cu K α , $\lambda = 1.5406 \text{ \AA}$). The film surface roughness (root mean square) was investigated with Dimension 3100 Nanoscope 3D (Veeco) atomic force microscope (AFM) under a tapping mode, and the surface roughness is an average value from five different locations for each sample. Room temperature Hall measurements were employed to determine the resistivity, mobility, and carrier concentration using the van der Pauw method (Ecopia HMS-3000), and the sheet resistance was measured using a four-point probe (surface resistivity meter SRM-232). Transmittance (*T*) and reflectance (*R*) were measured using UV/visible spectrophotometer (Lambda 950, Perkin-Elmer), and the direct optical bandgap was calculated from the α^2 versus *h* ν (photo energy) plot using the optical absorption coefficient α based on the *T* and *R*. The chemical state and the Fermi level shift of the films were investigated by X-ray photoelectron spectroscopy (XPS) (SSX-100 spectrometer, Surface Science Instruments), and all the XPS spectra reported here are referenced to C 1s peak at 284.5 eV with an accuracy of ± 0.1 eV (for SnO₂ peak, ± 0.2 eV).

3. Experimental results and discussion

Fig. 1(a) shows the XRD patterns obtained from as-grown and annealed ITO thin films. Crystallization was more apparent after annealing with diffraction peaks corresponding to (222), (400), (440), and (622) planes. The most prevalent peak was related to the (222) plane indicating a preferential orientation along this direction. All diffraction peaks were shifted to larger angles after annealing, which implies that there was a change in the residual strain between the lattice planes [11]. Interplanar spacing and grain size (calculated using the Scherrer formula) along the [222] direction as a function of temperature are shown in Fig. 1(b). The interplanar spacing gradually decreases after annealing, and it has a higher value than that of the well-known In₂O₃ powder's XRD interplanar spacing of 0.2921 nm [12] up to 400 °C. This indicates that extensive structural distortion dominates the stress in the crystallized films below 400 °C, and then compressive structural distortion dominates the films with increasing the post-annealing temperature and thermal stress. These results are found in good agreement with those reported by Guillen et al. [13] for sputtered and annealed ITO films on glass substrates. The change of interplanar spacing may be due to some oxygen that can leave the lattice at higher temperatures, resulting in a decrease of the lattice parameter [14]. Average grain size was not changed significantly with the post-annealing temperatures, so it is necessary to investigate the correlation between the grain size and mobility.

The effect of the post-annealing temperature on the surface morphology of the ITO films was investigated by AFM as shown in Fig. 2. Values of surface roughness are listed in Table 1. Although the surface roughness increases up to 400 °C and morphology of all annealed films is rougher than that of as-grown film, the grain size is not changed significantly which is consistent with XRD results.

This behavior may be due to less interaction with oxygen during annealing under nitrogen ambient, so the aggregation of the native grains into the larger clusters occurs [15], but the grain size itself is not affected.

Fig. 3 shows the dependence of the sheet resistance, resistivity, carrier concentration, and mobility of the ITO films on the post-annealing temperature. Although the mobility improves within the entire temperature range of 250–550 °C, the carrier concentration increases only up to 400 °C, leading to constant sheet and bulk resistivity for higher temperatures. With different batches under the same deposition and post-annealing conditions, the data showed a similar trend. The lowest measured resistivity of the films was $2.7 \times 10^{-4} \Omega \text{ cm}$ at 450 °C, and the highest mobility achieved was $40 \text{ cm}^2 \text{ V}^{-1} \text{ s}^{-1}$ at 550 °C. The mobility of a TCO is proportional to the relaxation time (τ) and inversely proportional to the electron effective mass (m_e^*) [16,17]. m_e^* of ITO films was calculated from an empirical equation:

$$m_e^* = (0.066 \times ne^{1/3} + 0.3) \times m_e, \quad (1)$$

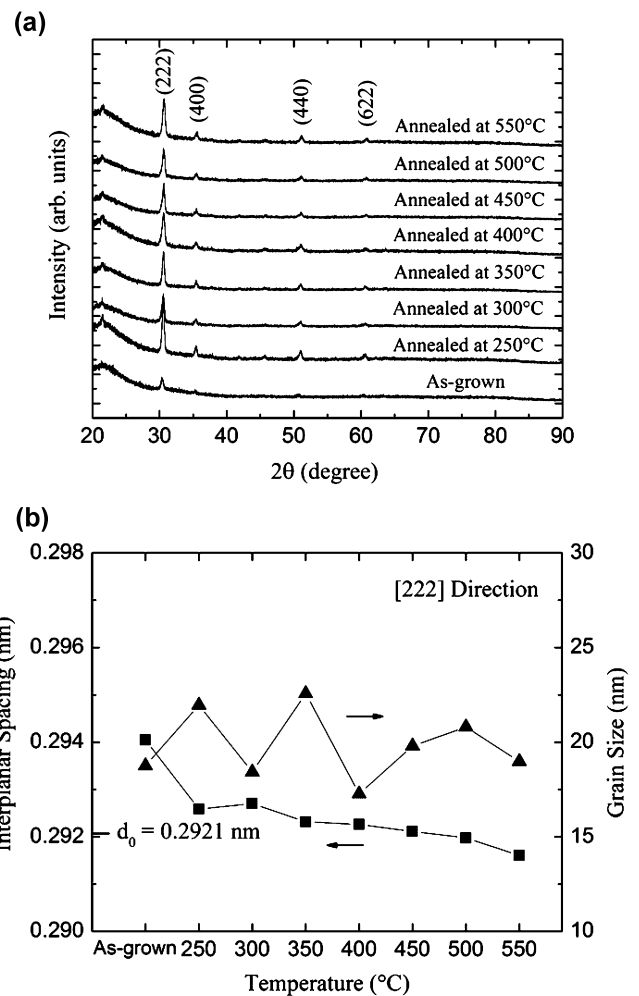


Fig. 1. (a) X-ray diffraction patterns of as-grown and annealed ITO thin films. (b) Interplanar spacing and grain size along the [222] direction as a function of the post-annealing temperature for the ITO films.

Download English Version:

<https://daneshyari.com/en/article/5351366>

Download Persian Version:

<https://daneshyari.com/article/5351366>

[Daneshyari.com](https://daneshyari.com)